Quasinormal modes of regular black holes

Antonino Flachi and José P. S. Lemos

Centro Multidisciplinar de Astrofísica - CENTRA,
Departamento de Física,
Instituto Superior Técnico - IST,
Universidade Técnica de Lisboa - UTL,
Av. Rovisco Pais 1, 1049-001 Lisboa, Portugal
Emails: antonino.flachi@ist.utl.pt, joselemos@ist.utl.pt
(Dated: June 7, 2018)

Black hole quasinormal frequencies are complex numbers that encode information on how a black hole relaxes after it has been perturbed and depend on the features of the geometry and on the type of perturbations. On the one hand, the examples studied so far in the literature focused on the case of black hole geometries with singularities in their interior. On the other hand, it is expected that quantum or classical modifications of general relativity may correct the pathological singular behavior of classical black hole solutions. Despite the fact that we do not have at hand a complete theory of quantum gravity, regular black hole solutions can be constructed by coupling gravity to an external form of matter, sometimes modeled by one form or another of nonlinear electrodynamics. It is therefore relevant to compute quasinormal frequencies for these regular solutions and see how differently, from the ordinary ones, regular black holes ring. In this paper, we take a step in this direction and, by computing the quasinormal frequencies, study the quasinormal modes of neutral and charged scalar field perturbations on regular black hole backgrounds in a variety of models.

I. INTRODUCTION

The problem of understanding how avoidance of singularities may be possible in general relativity goes beyond formal importance and is not at all new. In 1968 Bardeen constructed the first example of a regular black hole, i.e., a regular, nonsingular geometry with an event horizon, satisfying the weak energy conditions [1]. Despite its theoretical relevance, Bardeen's regular black hole solution lacked, for several years, a satisfactory physical interpretation. The reason is that it is not a vacuum solution of Einstein's equations and, in order to generate it, it is necessary to introduce some external form of matter or a modification to gravity. The solution was obtained by introducing an *ad hoc* energy momentum tensor, regular and bounded, decaying at infinity, and satisfying the weak energy conditions. However, no fundamental physical motivation for this choice had been given, until Ayon-Beato and Garcia reobtained the solution by describing it as the gravitational field of some sort of nonlinear magnetic monopole [2].

Bardeen's work has been followed by several other examples, motivating deeper analyses of how singularity avoidance may be possible in general. Other solutions have been proposed in the literature and some attention has been directed to theories of gravity coupled to nonlinear electrodynamics. Solutions have been discussed in different contexts, and a few of interest to us are, in addition to Refs. [1, 2], those analyzed in Refs. [3–8]. It is worth mentioning that an important viable example of a black hole with a regular center was constructed by Dymnikova, with a de Sitter core smoothly connecting to a Schwarzschild outer geometry [9]. Analysis of regular black hole solutions continued in several directions, see, e.g., Refs. [10, 11]. Another important step toward

understanding the absence of singularities in general relativity was taken by Borde who showed that, for a large class of black hole solutions, absence of singularities was related to a change in the topology beyond the event horizon [12]. Borde's arguments clearly demonstrated the impossibility of proving general singularity theorems when the strong energy condition or the existence of global hyperbolicity were not assumed.

Now, the interior is a hidden region by definition. The region that connects the interior to the exterior is the horizon and its near horizon region. Thus, a way to peer into the interior is to perturb the horizon. More important, quantum processes occur in its neighborhood, giving a glimpse of phenomena that unites quantum mechanics and gravitation. Indeed, the Hawking radiation has its origin in the vicinity of the horizon and the black hole entropy is believed to come out from degrees of freedom located at the horizon. Thus, the horizon is the region that may give a glimpse of what the black hole interior is. By poking the horizon something from the inside might pop up.

One way to poke the horizon is to perturb space-time, create quasinormal modes (QNMs), and analyze the result of the perturbation. Quasinormal frequencies (QNFs) are complex numbers that encode information on the system's relevant parameters and on its relaxation after it has been perturbed. Quasinormal modes are related to the classical evolution of a system. They can also reveal instability. A way to study QNMs is through a WKB approximation as was done first in [13]. This was further developed by Iyer and Will [14, 15] to study the Schwarzschild black hole and by [16–21] to study perturbation in the Reissner-Nordström case as well as charged scalar perturbations. Modes with large imaginary parts were analyzed, in connection with a possi-

ble horizon area quantization law, in Schwarzschild and Reissner-Nordström see [22, 23]. For reviews see [24–26].

All this work has been done for vacuum black holes. It is important to proceed for regular black holes. A first step was made by Fernando and Correa [27] who computed the QNFs for Bardeen's solution [1, 2]. In addition in Ref. [28] a study of the QNMs for the solution presented in [8] was performed. In this paper, we intend to study QNFs for the solutions given in Refs. [1–8].

II. SOME REGULAR BLACK HOLES

In the above context of gravity coupled to some form of matter, regular solutions were obtained from a prototypical action of the form

$$S = \frac{1}{16\pi} \int d^4x \sqrt{-g} \left(R - \mathscr{L} \right) , \qquad (1)$$

where g is the determinant of the metric $g_{\mu\nu}$, R is the scalar curvature, and $\mathscr{L}$ represents the Lagrangian of the matter fields. For the case of nonlinear electrodynamics then $\mathscr{L} = \mathscr{L}(F)$ is a nonlinear function of the electromagnetic field strength with $F = F_{\mu\nu}F^{\mu\nu}/4$.

The general line element

$$ds^2 = g_{\mu\nu}dx^\mu dx^\nu , \qquad (2)$$

when presented for spherically symmetric regular black hole solutions takes the form

$$ds^2 = -f(r)dt^2 + \frac{dr^2}{f(r)} + r^2 \left(d\theta^2 + \sin^2\theta \, d\phi^2 \right) , \quad (3)$$

where (t, r, θ, ϕ) are the usual space-time spherical coordinates and the lapse function $f \equiv f(r)$ depends on the specific form of underlying matter.

In [1] the function takes a particularly simple form

$$f(r) = 1 - \frac{2mr^2}{(r^2 + \alpha^2)^{3/2}} , \qquad (4)$$

with $\alpha = $ const and m being the mass of the solution. This implies a specific matter energy-momentum tensor that is de Sitter at the core and vanishes away at infinity as a magnetically charged solution in the context of a specific nonlinear electrodynamics with Lagrangian given by $\mathscr{L} = (3/(2s\alpha^2))(\sqrt{2\alpha^2 F}/(1 + \sqrt{2\alpha^2 F}))^{5/2}$, where $s = |\alpha|/2m$ and α is the magnetic charge [2]. Depending on the relative values of m and α, Eq. (5) can have two, one or zero horizons.

In [3] the function also takes a simple form

$$f(r) = 1 - \frac{2mr^2}{r^3 + 2\alpha^2} \qquad (5)$$

which is a variant from the original Bardeen's proposal [1] with $\alpha = $ constant. This also implies a specific matter energy-momentum tensor that is de Sitter at the core and vanishes away at infinity. As well, depending on the relative values of m and α equation (5) can have two, one or zero horizons [3].

The basic properties of the Lagrangian $\mathscr{L}(F)$ leading to electrically charged configurations have been discussed originally in Bronnikov [4, 5] and used by Dymnikova [6] to show that regular electrically charged solutions compatible with the weak energy condition require a de Sitter center and to construct a prototypical example. Specifically, Dymnikova's solution is obtained from a nonlinear electrodynamic theory with a Hamiltonian-like function (see [6] for details) of the form $\mathscr{H} = P \left(1 + \alpha\sqrt{-P} \right)^{-2}$, cwhere $P_{\mu\nu} = \mathscr{L}(F) F_{\mu\nu}$ $(P = P_{\mu\nu}P^{\mu\nu})$ leading to a solution of the above form with

$$f(r) = 1 - \frac{4m}{\pi r} \left(\tan^{-1}\frac{r}{r_0} - \frac{rr_0}{r^2 + r_0^2} \right) . \qquad (6)$$

The parameter r_0 in the solution (6) is a length scale related to the total mass m and the charge q by the relation $r_0 = \pi q^2/(8m)$. The above solution reproduces asymptotically, for $r \to \infty$, the Reissner-Nordström behavior, while near the center, for $r \ll r_0$ the solution approximates to de Sitter. Depending on the value of r_0, the above regular solution may present two distinct, one, or no horizons (see Fig. 1). Another electrically charged
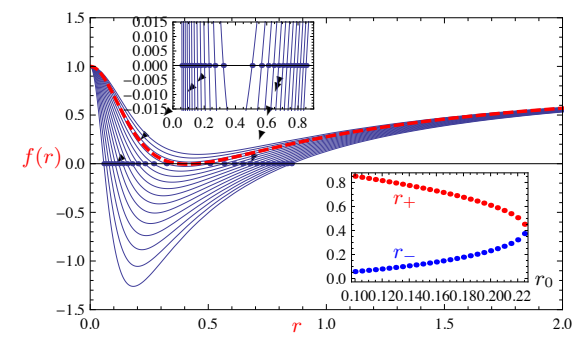

Figure 1. The behavior of the metric function $f(r)$ given in (6) for different values of the parameter r_0. The thick dashed line refers to the case where the two horizons overlap. The bottom-right inset represents the values of the outer (inner) horizon r_+ (r_-) vs the parameter r_0. The mass m has been normalized to unity and r_0 varied up to its critical value above which the horizons disappear and the geometry is regular.

solution discussed in the literature is the one presented by Ayon-Beato and García in Ref. [7]. It takes the form (3) with f given by

$$f = 1 - \frac{2mr^2}{(r^2 + q^2)^{3/2}} + \frac{q^2 r^2}{(r^2 + q^2)^2} , \qquad (7)$$

and it is obtained from a nonlinear electrodynamics with Lagrangian density $\mathscr{L} = \frac{X^2}{-2q^2}\frac{1-8X-3X^2}{(1-X)^4} - \frac{3m}{2q^3}\frac{X^{5/2}(3-2X)}{(1-X)^{7/2}}$, where $X = \sqrt{-2q^2 F}$, and m and q are associated with mass and charge, respectively. The above solution is asymptotically flat and behaves like Reissner-Nordström, at leading order, asymptotically. Depending on the values of the charge and mass, as Dymnikova's solution (6), it has two distinct inner and event horizons, for values of the charge smaller than a critical value q_c, two degenerate horizons for $q = q_c$, and becomes a globally

regular geometry for $q > q_c$. This solution, as discussed in Ref. [4], presents a problem related to the presence of cusps in the electromagnetic Lagrangian. As pointed out in Ref. [4], such a solution should be taken with care, and here we will use it as a useful working example and to check our numerics against known results.

Amongst the various models, the one of Ref. [8] is slightly more elaborate and the solution arises from the system of gravity coupled to a phantom scalar field.

All the solutions considered in this paper are summarized in Table I.

Lapse function	Ref.
$f(r) = 1 - \frac{2mr^2}{(r^2+\alpha^2)^{3/2}}$	[1, 2]
$f = 1 - \frac{2mr^2}{r^3+2\alpha^2}$	[3]
$f = 1 - \frac{2m}{r}\left(1 - \tanh\frac{r_0}{r}\right)$	[4, 5]
$f = 1 - \frac{4m}{\pi r}\left(\tan^{-1}\frac{r}{r_0} - \frac{rr_0}{r^2+r_0^2}\right)$	[6]
$f = 1 - \frac{2mr^2}{(r^2+q^2)^{3/2}} + \frac{q^2r^2}{(r^2+q^2)^2}$	[7]
$f = 1 + \frac{cr^2}{b^2} + \frac{\rho_0 r^2}{b^3}\left(\frac{b\sqrt{r^2-b^2}}{r^2} + \tan^{-1}\frac{\sqrt{r^2-b^2}}{b}\right)$	[8]

Table I. The models of Refs. [18] were constructed in such a way to have at least Reissner-Nordström asymptotics (i.e., order of $1 + 1/r + 1/r^\alpha$ with $\alpha \geq 2$, see Ref. [1,7]) or at least Reissner-Nordström-de Sitter asymptotics (i.e., order of $r^2 + 1/r + 1/r^\alpha$ with $\alpha \geq 2$, see Ref. [8] for the case $\alpha = 3$). The solution [1, 2] can be put in a nonlinear electrodynamics framework. The solution given in [3] is a minimal regular solution with the parameter m measuring the mass and the parameter α measuring the deviation of the nonsingular solution from Schwarzschild, which is reproduced for $\alpha = 0$. The models of Refs. [4–7] were constructed in the context of nonlinear electrodynamics coupled to gravity using different functional forms for $\mathscr{L}$. The parameter r_0 in [4–6] is a length scale related to the electric charge and q in [7] is the electric charge itself. The solution proposed in [8] was constructed coupling gravity to a phantom scalar field with a potential $U(b, c, \rho_0)$ where the parameters b, c, and ρ_0 characterize the features of the potential. All the details can be found in the original references.

III. QUASINORMAL FREQUENCIES

The computation of QNMs and their QNFs has been at the center of great attention both for the astrophysical relevance in relation to gravitational wave observation and for its formal importance. Extensive computations of QNFs for various black hole geometries are now available and most results have been reviewed [13–26].

Here we extend the computation of the QNFs to regular black hole geometries; see also [27, 28]. Although we will consider the specific solutions listed in Table I, it is worth noticing that the QNFs for uncharged scalar perturbations, as well as for tensor perturbations, depend on the specific form of the matter Lagrangian used to obtain the background solution only through the explicit functional form of the lapse function f. The same is also true for the case of charged scalar and vector perturbations,

as long as the weak field limit of the nonlinear electrodynamics reproduces the standard Maxwell's theory.

A. Neutral scalar perturbations

The computation of the QNFs for regular black hole geometries proceeds as in the well known cases, and this section will be devoted to those arising from neutral scalar field perturbations. The equation for these perturbations takes the usual form,

$$\frac{1}{\sqrt{g}}\partial_\mu\left(\sqrt{g}g^{\mu\nu}\partial_\nu\right)\phi = 0 , \tag{8}$$

where g is the determinant of the metric tensor $g_{\mu\nu}$ given in (3) and the lapse function f depends on the model considered. Equation (8) can be separated by decomposing the scalar perturbation into appropriate harmonics,

$$\phi = r^{-1}\sum_{lm} e^{-i\omega t}\varphi_{lm}(r)Y_l^m(\Omega) , \tag{9}$$

and by introducing the tortoise coordinate,

$$dx = dr/f .$$

One then can rewrite the radial part of (8) in a Schrödinger form,

$$\left[-\frac{d^2}{dx^2} + V(x) - \omega^2\right]\varphi(x) = 0 , \tag{10}$$

with V given by

$$V = f\left(\frac{\ell(\ell+1)}{r^2} + \frac{f'}{r}\right) , \tag{11}$$

and where the indices l, m have been suppressed from φ_{lm}. The boundary conditions, appropriate for the computation of the QNFs, must force the solution near the event horizon, $x = -\infty$ (at infinity, $x = +\infty$), not to generate outgoing (ingoing) waves. These can be written as
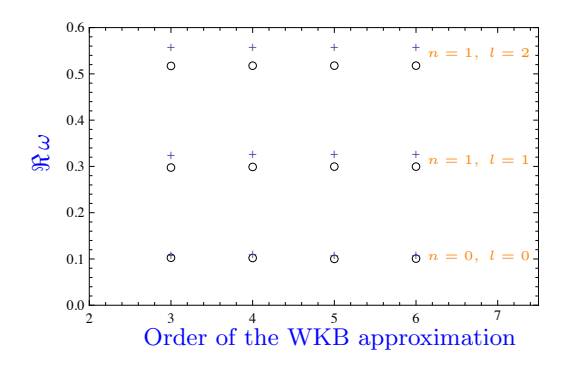
$$\varphi \sim e^{-i\omega x} , \quad x \to -\infty ,$$
$$\varphi \sim e^{+i\omega x} , \quad x \to +\infty .$$

In the present case, most available methods to compute QNFs would work.

Here, we will adopt the most direct way that makes use of WKB approximation, originally discussed in Ref. [14], and that does not require any special modification. Results for the quasinormal frequencies for neutral scalar perturbations are tabulated, in Appendix A, in Table II for the model given in Refs. [1, 2], in Table III for the model given in Ref. [3], in Table IV for the model given in Refs. [4, 5], in Table V for the model given in Ref. [6], in Table VI for the model given in Ref. [7], and in Table VII for the model given in Ref. [8]. The tables list the values of the frequencies at third order in the WKB approximation, as results to this order allow a direct comparison with the results presented in [15, 18]. One can go up to

sixth order in the WKB approximation and this allows to check the convergence of the approximation and how the accuracy improves going to higher order.

Figure 2 illustrates the real and imaginary parts of the frequencies for the solution of Dymnikova [6] and for sample values of the parameters, multipole number l, and overtone number n, up to sixth order WKB, thus allowing to test the convergence of the approximation.
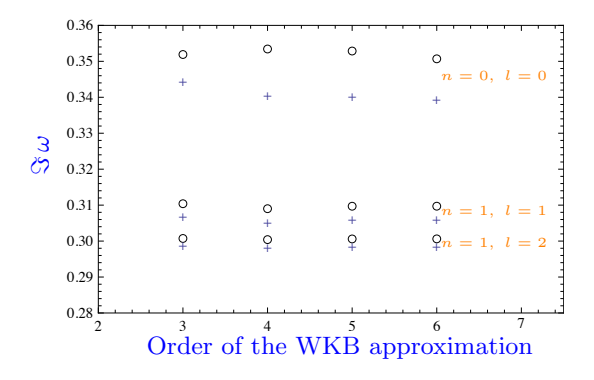

Figure 2. The real (upper panel) and imaginary (lower panel) parts of the QNFs from neutral scalar perturbations for sample values of the overtone and multipole numbers for the model of Dymnikova [6] when higher order terms in the WKB approximation are included in the computation. The symbols ○ (+) refer to $r_0 = 0.2$ ($r_0 = 0.3$) and we have normalized m to unity. The overtone and multipole numbers are indicated in the figure.

Because of its connection with a possible black hole area quantization law, it seems interesting to study the behavior of the QNFs in the limit of the large imaginary part. The problem is rather similar to the case of charged black hole solutions studied, for example, in Ref. [23]. This comes as no surprise, since the regular black hole solutions considered here have, at leading order, an asymptotic structure at least of the Reissner-Nordström type or Reissner-Nordström-de Sitter type, i.e., order of $1 + 1/r + 1/r^\alpha$ with $\alpha \geq 2$ (see [1,7]), or order of $r^2 + 1/r + 1/r^\alpha$ with $\alpha \geq 2$ (see [8] for the case $\alpha = 3$), respectively. Although formally the process of monodromy matching can be performed in the same way, one can see that in the limit $r \to 0$, the leading term

in the potential (11) behaves as $l(l + 1)r^{-2}$, rather than r^{-6}. This suggests that the QNFs, in the limit of the large imaginary part will depend on the multipole number l. Following the same steps as in [23], one finds that asymptotically the frequencies will satisfy the following relation:

$$e^{\beta\omega} = -(1 + 2\cos(\pi\sqrt{1 + l(l+1)}))$$
$$-e^{\beta_-\omega}(2 + 2\cos(\pi\sqrt{1 + l(l+1)})) , \quad (12)$$

where β and β_- are the inverse temperature at the outer and inner horizons. The above formula suggests that the real part of the QNFs does not asymptote to a constant value, nor display any periodic behavior. It may be interesting to study what happens in the extremal case. If the analogy with the Reissner-Nordström black hole is valid also in this case, then, as the charges approach the extremal value, the asymptotic value of the real part of the QNFs would spiral toward the asymptotic Schwarzschild QNFs [19, 20]. To test this, however, a more suitable numerical approach is necessary and this is left for future work.

B. Charged scalar perturbations

The computation of QNFs can be extended to charged scalar perturbations. The problem is similar to the Reissner-Nordström case treated in Refs. [16–19] where QNFs associated with charged scalar perturbations were computed. In particular, Ref. [18] followed the analysis of Ref. [17] that studied the evolution of scalar perturbations around collapsing charged black holes, indicating that scalar perturbations are radiated away, at a slower rate than the neutral ones, and follow an inverse power-law behavior at the future outer horizon, while displaying a decaying behavior accompanied by oscillations at the future outer horizon.

The general equation for the (complex) scalar perturbations can be written formally in the same way as [17],

$$\phi_{;ab}g^{ab} - ieA_a g^{ab}(2\phi_{;b} - ieA_b\phi) - ieA_{a;b}g^{ab}\phi = 0, (13)$$

with e being the (constant) charge of the scalar field. Since we are concerned with perturbations, the electromagnetic potential for the black hole is determined by the ordinary Maxwell's theory and can be written, up to an additive integration constant c, as

$$A_\mu dx^\mu = -\frac{q}{r}dt + c .$$

The integration constant is to be determined by regularity at the horizon for the gauge field. In fact, as far as the evaluation of the QNFs is concerned, its precise value is unessential since it would only produce a uniform shift in the real part of the frequencies. In the following, we will set $c = 0$. Equation (13) can be separated by decomposing the scalar perturbation into appropriate harmonics, and using tortoise coordinates it is possible to rewrite the

above equation in Schrödinger form,

$$\left[-\frac{d^2}{dx^2} + V(x) - (\omega + eq/r)^2 \right] \varphi(x) = 0 , \quad (14)$$

where V is given by (11). The boundary conditions relevant for the QNFs computation are

$$\varphi \sim e^{-i(\omega + eq/r_+)x} , \quad x \to -\infty ,$$
$$\varphi \sim e^{+i\omega x} , \quad x \to +\infty .$$

The WKB method works in this case too and the computation traces over the Reissner-Nordström case, with the difference being the lapse function $f(r)$, requiring a small adaptation in the numerics. In the case of charged perturbation some more work is necessary, but the same approach of analytic continuation used in Ref. [18] can be adopted here: first fix all the parameters including the multipole and overtone numbers, then maximize the potential as a function of the radial distance, and finally find the value of omega that satisfies the WKB relation for the QNFs as a numerical function analytically continued into the complex domain (the potential is generally a complex function). The results for the QNFs for charged scalar perturbations are listed in Appendix B, in Table VIII for the model given in Refs. [1, 2], in Table IX for the model in Ref. [9], and in Table X for the model in Ref. [7].

Figures 3 and 4 illustrate the behavior of the QNFs with respect to the charge q for the solution of [6]. It is possible to notice that for vanishing q the solution reproduces the Schwarschild geometry. In this limit, scalar perturbations become uncharged and the value of the QNFs must be smoothly connected with the QNFs for uncharged scalar perturbations on Schwarzschild black holes, indicated by the black dots in Figs. 3-4. Figures 5 and 6 illustrate the QNFs for the $l = 3$ and $n = 0$ mode for different values of the charge of the perturbation in the Reissner-Nordström case and in the regular black hole case. The choice of these specific values for the multipole and overtone numbers was motivated by the desire to compare our results with those of Ref. [18]. One notices (upper panel of Fig. 6) that the real part of the QNFs follows a behavior analogous to the Reissner-Nordström case; i.e., $\Re\omega$ grows with the charge and it is larger for charged perturbations than for neutral ones. This is a natural consequence of the fact that the regular black hole geometries considered asymptote, at leading order, to Reissner-Nordström. This indicates that, in the regular case as well, the late time behavior of the quasi-normal ringing will be dominated by the neutral scalar perturbations. The lower panel illustrates the imaginary part of the QNFs for Reissner-Nordström and for the regular black hole solution (3). While for small values of the charge q, i.e., in the region where the deviations from the two geometries are small, the values of $\Im\omega$ are basically superposed, the discrepancy increases with the charge signifying that in the large q region the exponential damping of these modes will occur less prominently
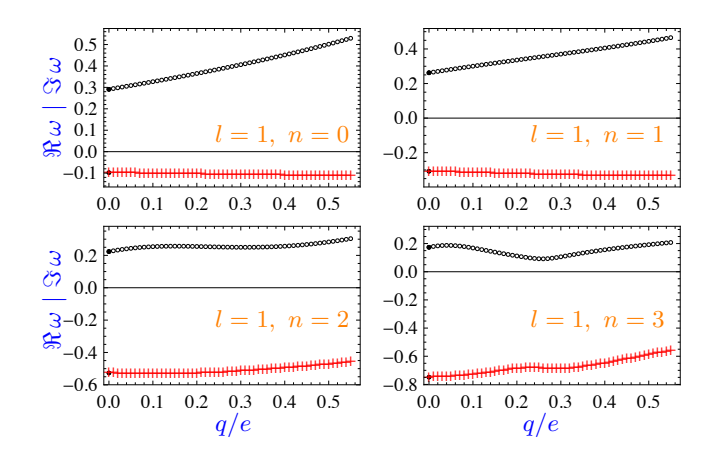

Figure 3. The real ($\circ$) and imaginary ($+$) parts of the QNFs with $l = 1$ from charged scalar perturbations for sample values of the overtone and multipole numbers (as indicated in the panels) for the model of Dymnikova [6]. The dark circles represent the values of the QNFs for the Schwarzschild case that are continuously connected with the values for the Dymnikova solution in the limit of zero charge ($q = 0$).
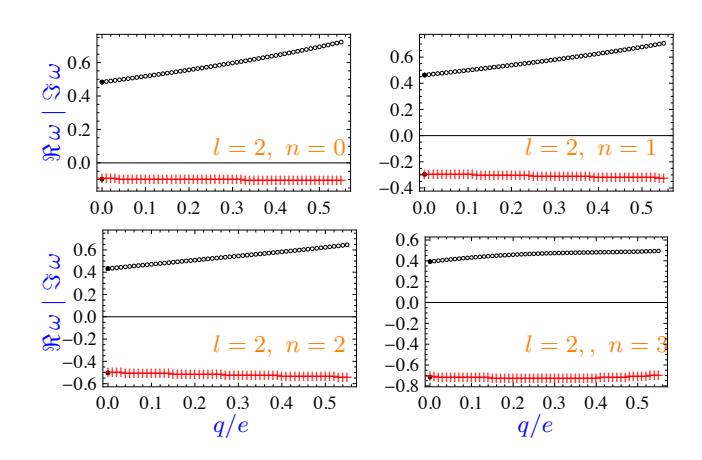
Figure 4. Same as Fig. 3 with $l = 2$.

than in the Reissner-Nordström case. The coincidence in the imaginary parts of the QNFs is observed in the regular case as well, but the feature of the profile, namely the fact that $\Im\omega$ undergoes a transient increase before dropping for large values of the charge, is much less prominent in the regular case, where the increase in $\Im\omega$ for moderate values of q is small.

IV. CONCLUSIONS

In this work we have computed the neutral and charged scalar QNFs for regular black hole geometries. The prototype example of such regular solutions is the one proposed by Bardeen many years ago [1] (see also [2]), and

Figure 5. The behavior of the real part of the QNFs for $l = 3$ and $n = 0$ in the Reissner-Nordström case and in the regular black hole case for the model given in [7], see Eq. (7). The symbols refer to $q = 0\,(+)$, $0.1\,(\sharp)$, $0.3\,(*)$ for the regular case, and $q = 0\,(\flat)$, $0.1\,(\natural)$, $0.3\,(\Delta)$ for the Reissner-Nordström case.
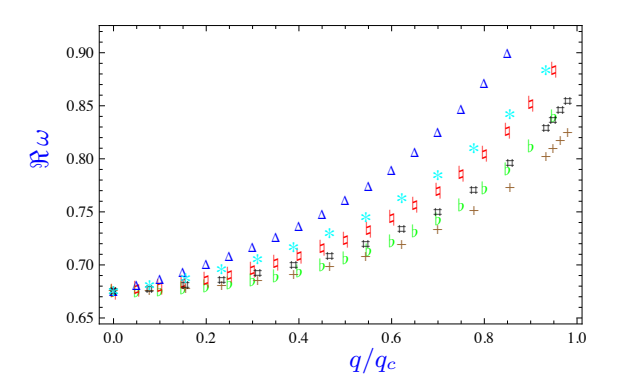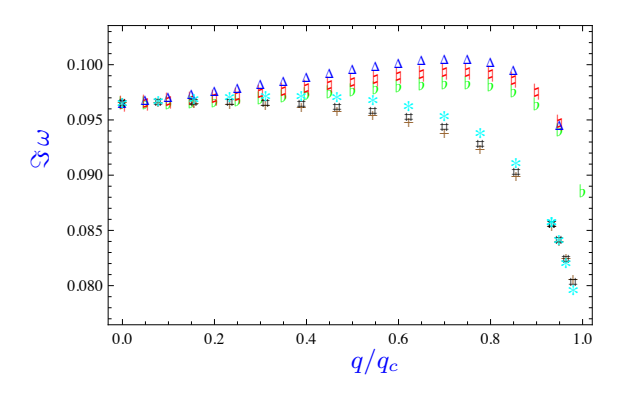

Figure 6. Same as Fig. 5 for the imaginary part of the QNFs.

being perturbed can shed light on some fundamental aspects of quantum gravity. In turn, knowledge of quantum gravity should provide us with a better understanding of black holes and eventually suggest a possible resolution of the singularity problem. In fact, the presence of singularities certainly signals a limitation of our understanding, if not a breakdown, of general relativity. This pathological behavior is usually believed to disappear in a full theory of quantum gravity that would provide a consistent framework to test the well known semiclassical arguments predicting the evaporation of black holes.

several examples were constructed following this original example. Such solutions are spherically symmetric, multihorizon, and singularity-free and display an asymptotic behavior analogous, at leading order, to at least Reissner-Nordström or Reissner-Nordström-de Sitter, while having a near-horizon behavior similar to Schwarzschild. The WKB method can be implemented in the present case, and it has been adopted to compute the QNFs for the variety of models of Refs. [1–8]. The results have been tested in the limit of Schwarzschild and Reissner-Nordström black holes reproducing the known results of Refs.[15, 18] when the same order in the WKB approximation is used and the convergence has been tested up to sixth order in the WKB expansion. The QNMs of Bardeen's model have also been studied in [27, 28].

Aside of the generalization to other types of perturbations, the use of more sophisticated numerical methods, like those used in Ref. [19], may be useful to check the accuracy of the WKB approximation as well we to test the asymptotic behavior of the QNFs. These problems are left for future work.

Certainly, knowledge of how a black hole rings after

Appendix A: Tables of QNFs for neutral scalar perturbations

l	n	$q = 0.1$	$q = 0.3$	$q = 0.6$
0	0	$0.1049 - \imath\, 0.1149$	$0.1070 - \imath\, 0.1125$	$0.1093 - \imath\, 0.1015$
	1	$0.0895 - \imath\, 0.3541$	$0.0921 - \imath\, 0.3473$	$0.0866 - \imath\, 0.3219$
1	0	$0.2916 - \imath\, 0.0978$	$0.2959 - \imath\, 0.0967$	$0.3132 - \imath\, 0.0906$
	1	$0.2629 - \imath\, 0.3069$	$0.2686 - \imath\, 0.3028$	$0.2886 - \imath\, 0.2820$
	2	$0.2245 - \imath\, 0.5259$	$0.2323 - \imath\, 0.5187$	$0.2548 - \imath\, 0.4831$
	3	$0.1750 - \imath\, 0.7474$	$0.1860 - \imath\, 0.7368$	$0.2125 - \imath\, 0.6869$
2	0	$0.4840 - \imath\, 0.0966$	$0.4909 - \imath\, 0.0956$	$0.5191 - \imath\, 0.0901$
	1	$0.4641 - \imath\, 0.2954$	$0.4721 - \imath\, 0.2920$	$0.5034 - \imath\, 0.2740$
	2	$0.4328 - \imath\, 0.5027$	$0.4424 - \imath\, 0.4966$	$0.4777 - \imath\, 0.4645$
	3	$0.3940 - \imath\, 0.7148$	$0.4058 - \imath\, 0.7059$	$0.4454 - \imath\, 0.6595$

Table II. QNFs for neutral scalar perturbations for $q = 0.1$, 0.3, 0.6 and $m = 1$ for the model of Refs. [1, 2]. The model reproduces the original example constructed by Bardeen using a nonlinear electromagnetic theory that displays, in the weak field limit, a stronger behavior as compared to the ordinary Maxwell's one. In this model the gravitational field can be interpreted as that of a nonlinear magnetic monopole.

l	n	$\alpha = 0.1$	$\alpha = 0.4$	$\alpha = 0.7$
0	0	$0.1046 - \imath\, 0.1148$	$0.1034 - \imath\, 0.1093$	$0.0923 - \imath\, 0.0986$
	1	$0.0891 - \imath\, 0.3541$	$0.0835 - \imath\, 0.3424$	$0.0562 - \imath\, 0.3281$
1	0	$0.2913 - \imath\, 0.0978$	$0.2946 - \imath\, 0.0948$	$0.3018 - \imath\, 0.0854$
	1	$0.2624 - \imath\, 0.3068$	$0.2655 - \imath\, 0.2973$	$0.2649 - \imath\, 0.2691$
	2	$0.2238 - \imath\, 0.5258$	$0.2264 - \imath\, 0.5104$	$0.2108 - \imath\, 0.4677$
	3	$0.1741 - \imath\, 0.7473$	$0.1764 - \imath\, 0.7262$	$0.1418 - \imath\, 0.6727$
2	0	$0.4835 - \imath\, 0.0966$	$0.4892 - \imath\, 0.0940$	$0.5037 - \imath\, 0.0855$
	1	$0.4636 - \imath\, 0.2953$	$0.4700 - \imath\, 0.2870$	$0.4823 - \imath\, 0.2601$
	2	$0.4321 - \imath\, 0.5025$	$0.4392 - \imath\, 0.4881$	$0.4445 - \imath\, 0.4422$
	3	$0.3931 - \imath\, 0.7146$	$0.4009 - \imath\, 0.6942$	$0.3946 - \imath\, 0.6310$

Table III. QNFs for neutral scalar perturbations $\alpha = 0.1$, 0.4, 0.6 and $m = 1$ for the solution of Refs. [3].

l	n	$r_0 = 0.1$	$r_0 = 0.3$	$r_0 = 0.4$
0	0	$0.1091 - \imath\, 0.1151$	$0.1189 - \imath\, 0.1119$	$0.1200 - \imath\, 0.1065$
	1	$0.0940 - \imath\, 0.3550$	$0.1021 - \imath\, 0.3482$	$0.0940 - \imath\, 0.3401$
1	0	$0.3019 - \imath\, 0.0988$	$0.3303 - \imath\, 0.0990$	$0.3503 - \imath\, 0.0962$
	1	$0.2742 - \imath\, 0.3094$	$0.3058 - \imath\, 0.3080$	$0.3252 - \imath\, 0.2980$
	2	$0.2374 - \imath\, 0.5297$	$0.2729 - \imath\, 0.5264$	$0.2897 - \imath\, 0.5098$
	3	$0.1902 - \imath\, 0.7523$	$0.2319 - \imath\, 0.7472$	$0.2451 - \imath\, 0.7249$
2	0	$0.5007 - \imath\, 0.0977$	$0.5472 - \imath\, 0.0982$	$0.5810 - \imath\, 0.0957$
	1	$0.4815 - \imath\, 0.2984$	$0.5306 - \imath\, 0.2990$	$0.5652 - \imath\, 0.2904$
	2	$0.4514 - \imath\, 0.5074$	$0.5041 - \imath\, 0.5071$	$0.5387 - \imath\, 0.4916$
	3	$0.4141 - \imath\, 0.7212$	$0.4715 - \imath\, 0.7199$	$0.5051 - \imath\, 0.6976$

Table IV. QNFs for neutral scalar perturbations for $r_0 = 0.1$, 0.3, 0.4 for the solution of Refs. [4, 5]. This solution is obtained in the context of gravity plus nonlinear electrodynamics [4]. The solution has also been extended to the case when higher order curvature corrections are included in the gravitational action Ref. [5]. The parameter r_0 is a length scale related to the charge.

l	n	$r_0 = 0.1$	$r_0 = 0.3$	$r_0 = 0.4$
0	0	$0.1104 - \imath\, 0.1150$	$0.1241 - \imath\, 0.1104$	$0.1275 - \imath\, 0.1030$
	1	$0.0954 - \imath\, 0.3548$	$0.1073 - \imath\, 0.3440$	$0.0993 - \imath\, 0.3314$
1	0	$0.3051 - \imath\, 0.0991$	$0.3452 - \imath\, 0.0989$	$0.3771 - \imath\, 0.0940$
	1	$0.2779 - \imath\, 0.3098$	$0.3227 - \imath\, 0.3065$	$0.3549 - \imath\, 0.2896$
	2	$0.2416 - \imath\, 0.5303$	$0.2924 - \imath\, 0.5232$	$0.3220 - \imath\, 0.4940$
	3	$0.1953 - \imath\, 0.7531$	$0.2550 - \imath\, 0.7422$	$0.2806 - \imath\, 0.7021$
2	0	$0.5060 - \imath\, 0.0980$	$0.5716 - \imath\, 0.0982$	$0.6254 - \imath\, 0.0936$
	1	$0.4871 - \imath\, 0.2990$	$0.5564 - \imath\, 0.2984$	$0.6119 - \imath\, 0.2834$
	2	$0.4573 - \imath\, 0.5083$	$0.5321 - \imath\, 0.5054$	$0.5885 - \imath\, 0.4783$
	3	$0.4207 - \imath\, 0.7224$	$0.5023 - \imath\, 0.7170$	$0.5583 - \imath\, 0.6775$

Table V. QNFs for neutral scalar perturbations for $r_0 = 0.1,\ 0.3,\ 0.4$ and $m = 1$ for the model of Ref. [6].

l	n	$q = 0$	$q = 0.3$	$q = 0.6$
0	0	$0.1046 - \imath\, 0.1152$	$0.1089 - \imath\, 0.1123$	$0.1118 - \imath\, 0.0970$
	1	$0.0892 - \imath\, 0.3549$	$0.0940 - \imath\, 0.3470$	$0.0804 - \imath\, 0.3177$
1	0	$0.2911 - \imath\, 0.0980$	$0.3009 - \imath\, 0.0970$	$0.3424 - \imath\, 0.0861$
	1	$0.2622 - \imath\, 0.3074$	$0.2742 - \imath\, 0.3034$	$0.3153 - \imath\, 0.2667$
	2	$0.2235 - \imath\, 0.5268$	$0.2386 - \imath\, 0.5195$	$0.2737 - \imath\, 0.4581$
	3	$0.1737 - \imath\, 0.7486$	$0.1934 - \imath\, 0.7378$	$0.2207 - \imath\, 0.6545$
2	0	$0.4832 - \imath\, 0.0968$	$0.4990 - \imath\, 0.0960$	$0.5689 - \imath\, 0.0858$
	1	$0.4631 - \imath\, 0.2958$	$0.4806 - \imath\, 0.2929$	$0.5531 - \imath\, 0.2599$
	2	$0.4316 - \imath\, 0.5034$	$0.4515 - \imath\, 0.4979$	$0.5248 - \imath\, 0.4393$
	3	$0.3925 - \imath\, 0.7158$	$0.4158 - \imath\, 0.7076$	$0.4871 - \imath\, 0.6236$

Table VI. QNFs for neutral scalar perturbations for the model of Ref. [7]. The $q = 0$ values reproduce those of Ref. [15] for the Schwarzschild case.

l	n	$b = 0.1$	$b = 0.5$	$b = 1$
0	0	$0.1045 - \imath\, 0.1152$	$0.1032 - \imath\, 0.1166$	$0.0989 - \imath\, 0.1210$
	1	$0.0891 - \imath\, 0.3551$	$0.0872 - \imath\, 0.3590$	$0.0811 - \imath\, 0.3716$
1	0	$0.2910 - \imath\, 0.0980$	$0.2885 - \imath\, 0.0986$	$0.2813 - \imath\, 0.1006$
	1	$0.2620 - \imath\, 0.3075$	$0.2587 - \imath\, 0.3097$	$0.2489 - \imath\, 0.3167$
	2	$0.2233 - \imath\, 0.5269$	$0.2186 - \imath\, 0.5309$	$0.2047 - \imath\, 0.5431$
	3	$0.1734 - \imath\, 0.7488$	$0.1667 - \imath\, 0.7546$	$0.1466 - \imath\, 0.7724$
2	0	$0.6749 - \imath\, 0.0965$	$0.4791 - \imath\, 0.0973$	$0.4677 - \imath\, 0.0990$
	1	$0.6601 - \imath\, 0.2924$	$0.4584 - \imath\, 0.2976$	$0.4451 - \imath\, 0.3031$
	2	$0.6345 - \imath\, 0.4942$	$0.4259 - \imath\, 0.5068$	$0.4095 - \imath\, 0.5166$
	3	$0.6018 - \imath\, 0.7012$	$0.3854 - \imath\, 0.7208$	$0.3648 - \imath\, 0.7351$

Table VII. QNFs for neutral scalar perturbations for the solution of Ref. [8] obtained for a system of gravity coupled to a phantom scalar field. The parameters have been fixed in order to normalize to unity the black hole mass, $c = -3\pi/(2b)$ and $\rho_0 = 3$ and b has been set to $b = 0.1,\ 0.5, 1$.

Appendix B: Tables of QNFs for charged scalar perturbations

l	n	$q = 0.1$	$q = 0.2$	$q = 0.3$
0	0	$0.1451 - \imath\, 0.1198$	$0.1895 - \imath\, 0.1224$	$0.2393 - \imath\, 0.1219$
	1	$0.0730 - \imath\, 0.3454$	$0.0479 - \imath\, 0.3027$	$0.0683 - \imath\, 0.2577$
1	0	$0.3267 - \imath\, 0.1011$	$0.3655 - \imath\, 0.1036$	$0.4082 - \imath\, 0.1051$
	1	$0.3005 - \imath\, 0.3144$	$0.3369 - \imath\, 0.3189$	$0.3729 - \imath\, 0.3200$
	2	$0.2540 - \imath\, 0.5292$	$0.2517 - \imath\, 0.5192$	$0.2479 - \imath\, 0.4841$
	3	$0.1635 - \imath\, 0.7248$	$0.0923 - \imath\, 0.6242$	$0.0938 - \imath\, 0.5115$
2	0	$0.5182 - \imath\, 0.0987$	$0.5564 - \imath\, 0.1002$	$0.5987 - \imath\, 0.1012$
	1	$0.5000 - \imath\, 0.3012$	$0.5397 - \imath\, 0.3051$	$0.5831 - \imath\, 0.3071$
	2	$0.4708 - \imath\, 0.5106$	$0.5096 - \imath\, 0.5151$	$0.5488 - \imath\, 0.5167$
	3	$0.4323 - \imath\, 0.7219$	$0.4607 - \imath\, 0.7238$	$0.4791 - \imath\, 0.7197$

Table VIII. QNFs for charged scalar perturbations and for the solution of Ref. [1, 2]. We normalized m and e to unity.

l	n	$q = 0.1$	$q = 0.2$	$q = 0.3$
0	0	$0.1447 - \imath\, 0.1201$	$0.1895 - \imath\, 0.1247$	$0.2383 - \imath\, 0.1251$
	1	$0.0724 - \imath\, 0.3463$	$0.1684 - \imath\, 0.3435$	$0.1368 - \imath\, 0.2724$
1	0	$0.3266 - \imath\, 0.1013$	$0.3647 - \imath\, 0.1044$	$0.4060 - \imath\, 0.1072$
	1	$0.3002 - \imath\, 0.3150$	$0.3355 - \imath\, 0.3216$	$0.3690 - \imath\, 0.3266$
	2	$0.2535 - \imath\, 0.5303$	$0.2500 - \imath\, 0.5222$	$0.2407 - \imath\, 0.4907$
	3	$0.1626 - \imath\, 0.7262$	$0.0926 - \imath\, 0.6279$	$0.0871 - \imath\, 0.5162$
2	0	$0.5181 - \imath\, 0.0989$	$0.5559 - \imath\, 0.1010$	$0.5972 - \imath\, 0.1031$
	1	$0.4998 - \imath\, 0.3017$	$0.5388 - \imath\, 0.3075$	$0.5807 - \imath\, 0.3132$
	2	$0.4705 - \imath\, 0.5116$	$0.5081 - \imath\, 0.5193$	$0.5448 - \imath\, 0.5268$
	3	$0.4317 - \imath\, 0.7234$	$0.4581 - \imath\, 0.7295$	$0.4721 - \imath\, 0.7322$

Table IX. QNFs for charged scalar perturbations and for the solution of Ref. [6]. We normalized m and e to unity.

l	n	$q = 0.1$	$q = 0.2$	$q = 0.3$
0	0	$0.1459 - \imath\, 0.1199$	$0.1929 - \imath\, 0.1224$	$0.2473 - \imath\, 0.1215$
	1	$0.0874 - \imath\, 0.3515$	$0.0526 - \imath\, 0.3059$	$0.0703 - \imath\, 0.2557$
1	0	$0.3275 - \imath\, 0.1012$	$0.3689 - \imath\, 0.1038$	$0.4175 - \imath\, 0.1054$
	1	$0.3014 - \imath\, 0.3145$	$0.3407 - \imath\, 0.3194$	$0.3828 - \imath\, 0.3227$
	2	$0.2559 - \imath\, 0.5292$	$0.2573 - \imath\, 0.5199$	$0.2462 - \imath\, 0.4930$
	3	$0.1704 - \imath\, 0.7238$	$0.1008 - \imath\, 0.6282$	$0.0830 - \imath\, 0.5105$
2	0	$0.5192 - \imath\, 0.0988$	$0.5609 - \imath\, 0.1004$	$0.6103 - \imath\, 0.1015$
	1	$0.5010 - \imath\, 0.3013$	$0.5443 - \imath\, 0.3056$	$0.5951 - \imath\, 0.3080$
	2	$0.4719 - \imath\, 0.5108$	$0.5145 - \imath\, 0.5160$	$0.5620 - \imath\, 0.5184$
	3	$0.4335 - \imath\, 0.7222$	$0.4660 - \imath\, 0.7249$	$0.4943 - \imath\, 0.7257$

Table X. QNFs for charged scalar perturbations and for the solution of Ref. [7]. We normalized m and e to unity.

[1] J.M. Bardeen, *Proceedings of GR5* (Tbilisi, USSR, 1968), p. 174.
[2] E. Ayon-Beato and A. Garcia, Phys. Lett. B **493**, 149 (2000).
[3] S. A. Hayward, Phys. Rev. Lett. **96**, 031103 (2006).
[4] K. A. Bronnikov, Phys. Rev. D **63**, 044005 (2001).
[5] W. Berej, J. Matyjasek, D. Tryniecki and M. Woronowicz, Gen. Relativ. Gravit. **38**, 885 (2006).
[6] I. Dymnikova, Classical Quantum Gravity **21**, 4417 (2004).
[7] E. Ayón-Beato and A. García, Phys. Rev. Lett. **80**, 5056 (1998).
[8] K. A. Bronnikov and J. C. Fabris, Phys. Rev. Lett. **96**, 251101 (2006).
[9] I. Dymnikova, Gen. Relativ. Gravit. **24**, 235 (1992).
[10] S. Ansoldi, arXiv:0802.0330 [gr-qc].
[11] J. P. S. Lemos and V. T. Zanchin, Phys. Rev. D **83**, 124005 (2011).
[12] A. Borde, Phys. Rev. D **55**, 7615 (1997).
[13] B. F. Schutz and C. M. Will, Astrophys. J. **291**, L33 (1985).
[14] S. Iyer and C. M. Will, Phys. Rev. D **35**, 3621 (1987).
[15] S. Iyer, Phys. Rev. D **35**, 3632 (1987).
[16] E.W. Leaver, Phys. Rev. D **41**, 2986 (1990).
[17] S. Hod and T. Piran, Phys. Rev. D **58**, 024017 (1998).
[18] R. A. Konoplya, Phys. Rev. D **66**, 084007 (2002).
[19] E. Berti and K. D. Kokkotas, Phys. Rev. D **68**, 044027 (2003).
[20] A. Neitzke, arXiv:hep-th/0304080.
[21] R. A. Konoplya and A. Zhidenko, Rev. Mod. Phys. **83**, 793 (2011).
[22] L. Motl, Adv. Theor. Math. Phys. **6**, 1135 (2003).
[23] L. Motl and A. Neitzke, Adv. Theor. Math. Phys. **7**, 307 (2003).
[24] H. P. Nollert, Classical Quantum Gravity **16**, R159 (1999).
[25] K. D. Kokkotas and B. G. Schmidt, Living Rev. Relativity **2**, 2 (1999).
[26] E. Berti, V. Cardoso and A. O. Starinets, Classical Quantum Gravity **26**, 163001 (2009).
[27] S. Fernando and J. Correa, Phys. Rev. D **86** (2012) 064039
[28] K. A. Bronnikov, R. A. Konoplya and A. Zhidenko, Phys. Rev. D **86** (2012) 024028